Potential Flow.

-Elementary Plane-flow solutions

Three types of elementary solutions.

(1). Uniform stream

(2). Source or sink

(3) Vortex.

The potential and stream functions can be added to produce various useful results. In doing this we rely on the principle of superposition.

Uniform stream.

A stream of constant velocity U_∞ has zero spatial derivatives and hence satisfies continuity and irrotationality identically

$$u = U_\infty = \frac{\partial \psi}{\partial y} = \frac{\partial \phi}{\partial x} = \text{const.}$$

$$v = 0 = -\frac{\partial \psi}{\partial x} = \frac{\partial \phi}{\partial y} \qquad (1)$$

integrating.

$$\psi = U_\infty y + C_1 \qquad \phi = U_\infty x + C_2$$

C_1 an C_2 no effect whatever no velocities or pressure in the flow.

$\psi = V_\infty y \qquad \phi = V_\infty x \qquad (2)$

These are plotted in Figure. 1

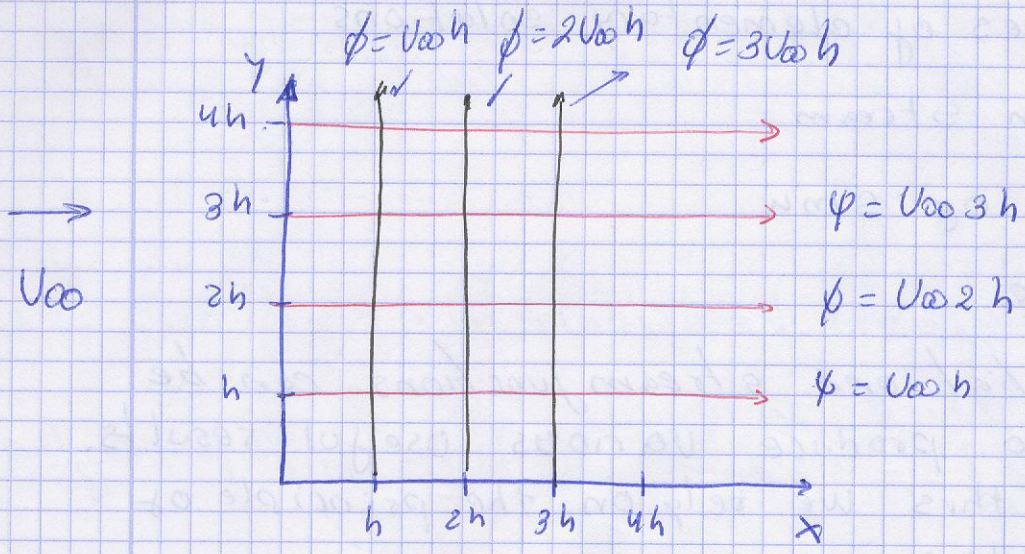

Figure 1

In terms of polar coordinates

$\psi = V_\infty r \sin\theta \qquad \phi = V_\infty r \cos\theta$

We generalize to a uniform stream angle

$$u = V_\infty \cos\alpha = \frac{\partial \psi}{\partial y} = \frac{\partial \phi}{\partial x}$$

$$v = V_\infty \sin\alpha = -\frac{\partial \psi}{\partial x} = \frac{\partial \phi}{\partial y}$$

Integrating

$$\psi = V_\infty (y\cos\alpha - x\sin\alpha)$$

$$\phi = V_\infty (x\cos\alpha + y\sin\alpha)$$

useful in airfoil angle of attack problems.

- Line Source or Sink

Suppose that the z-axis were a sort of thin pipe manifold through which fluid issued at a uniform rate along its length.

In steady flow the amount of fluid crossing any given cylindrical surface of radius r and length b is constant

$$Q = V_r (2\pi r b) = \text{constant} = 2\pi b m.$$

where $\frac{m}{r} = V_r$, source where m is a convenient constant. this is called a line source if (m) is positive and sink if (m) is negative

We have

$$V_r = \frac{m}{r} = \frac{1}{r}\frac{\partial \psi}{\partial \theta} = \frac{\partial \phi}{\partial r} \qquad V_\theta = 0 = -\frac{\partial \psi}{\partial r} = \frac{1}{r}\frac{\partial \phi}{\partial \theta}$$

Integrating

$$\psi = m\theta \qquad \phi = m \ln r \qquad (3)$$

For cartesian coordinates.

$$\psi = m \tan^{-1}\left(\frac{y}{x}\right) \qquad \phi = m \ln \sqrt{(x^2 + y^2)}$$

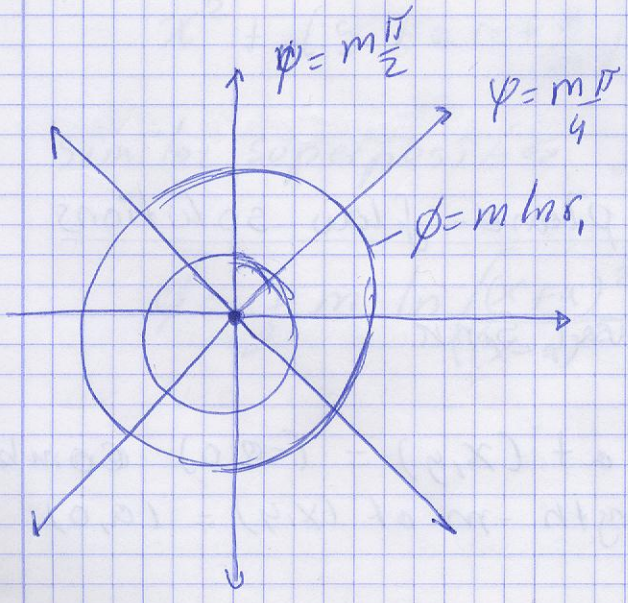

Line source Figure 2

Line vortex.

Now suppose we reverse the roles of ψ and ϕ in equation (3).

κ is the vortex strength.

$$\psi = -\kappa \ln r \qquad \phi = \kappa\theta \qquad (4)$$

by direct differentiation of either one we obtain the velocity pattern.

$$V_r = 0 \qquad V_\theta = \frac{\kappa}{r} \qquad (5)$$

This is a purely circulating flow with tangential velocity dropping off as $\frac{1}{r}$

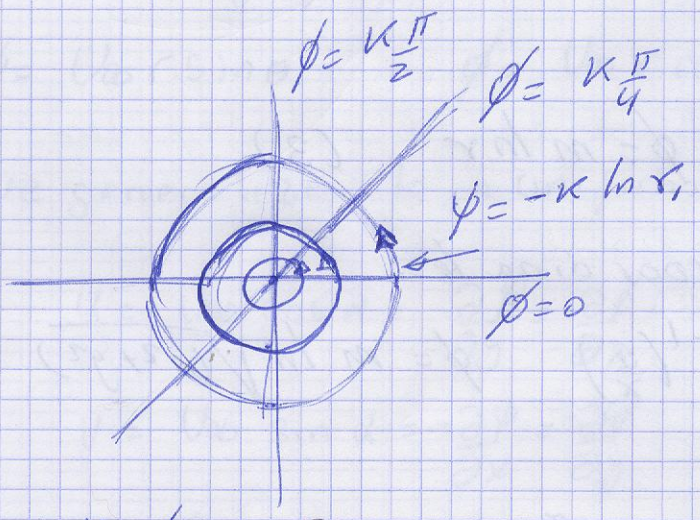

Vortex Figure 3

Superposition of plane-flow solutions

Source plus and equal Sink

Source strength m at $(x,y) = (-a,0)$ combined with a sink of strength $-m$ at $(x,y) = (a,0)$

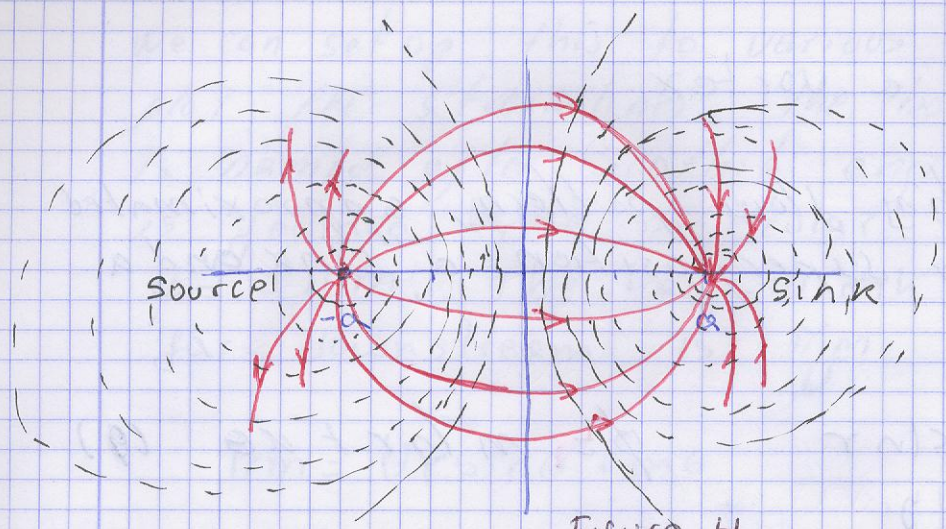

Figure 4

$\psi = \psi_{source} + \psi_{sink}$ ~~$\psi_{source} + \psi_{sink}$~~

$$m \tan^{-1}\left(\frac{y}{x+a}\right) - m \tan^{-1}\left(\frac{y}{x-a}\right) \qquad (6)$$

Trigonometric identity

$$\tan^{-1}\alpha - \tan^{-1}\beta = \tan^{-1}\left(\frac{\alpha-\beta}{1+\alpha\beta}\right)$$

we write (6) as

$$\psi = -m \tan^{-1}\left(\frac{2ay}{x^2+y^2-a^2}\right) \qquad (7)$$

rearranged to exhibit the functional form.

$$x^2 + \left(y + a\cot\frac{\psi}{m}\right)^2 = a^2 \csc^2\frac{\psi}{m}$$

similar superposition for velocity potential

$$\phi = \frac{1}{2} m \ln\left(\frac{(x+a)^2+y^2}{(x-a)^2+y^2}\right) \qquad (8)$$

Sink plus a vortex

An interesting flow pattern, approximated in nature by superposition a sink and a vortex.

$$\psi = -m\theta - k\ln r \qquad \phi = m\ln r + k\theta \quad (9)$$

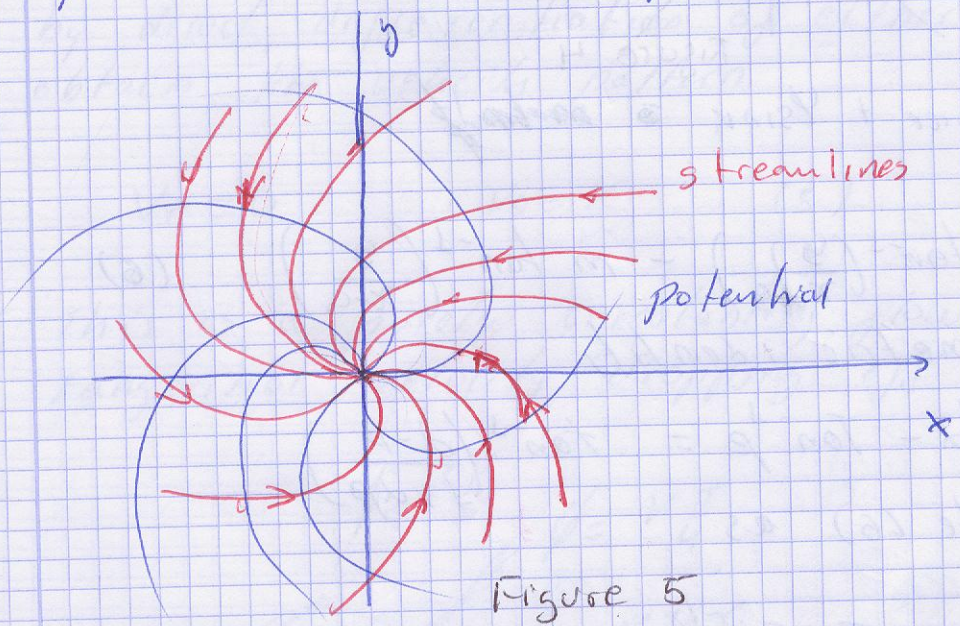

Figure 5

This a realistic simulation of a tornado (where the sink flow moves up the z-axis into atmosphere) or a rapidly draining bathtub vortex.

- Uniform Stream plus a source at origin (Rankine Half-body).

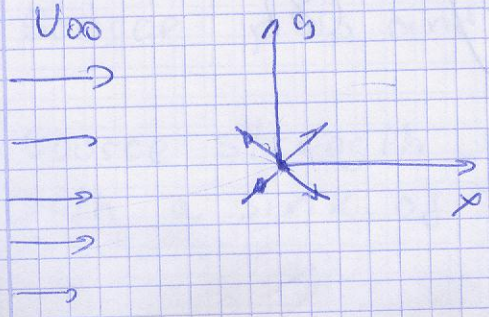

$$\psi = Ur\sin\theta + m\theta \quad (10)$$

stream flow at polar coordinate

source at polar coordinate

We can set up this to various constants and plot the streamlines. The body shape, which is named after Scottish engineer W.J.M Rankine, is formed by a particular streamlines: $\psi = \pm \pi m$. The half-width of the body far downstream is $\frac{\pi m}{U}$

$$\pi m = U r \sin\theta + m\theta$$

$$\frac{m(\pi - \theta)}{U \sin\theta} = r \qquad (11)$$

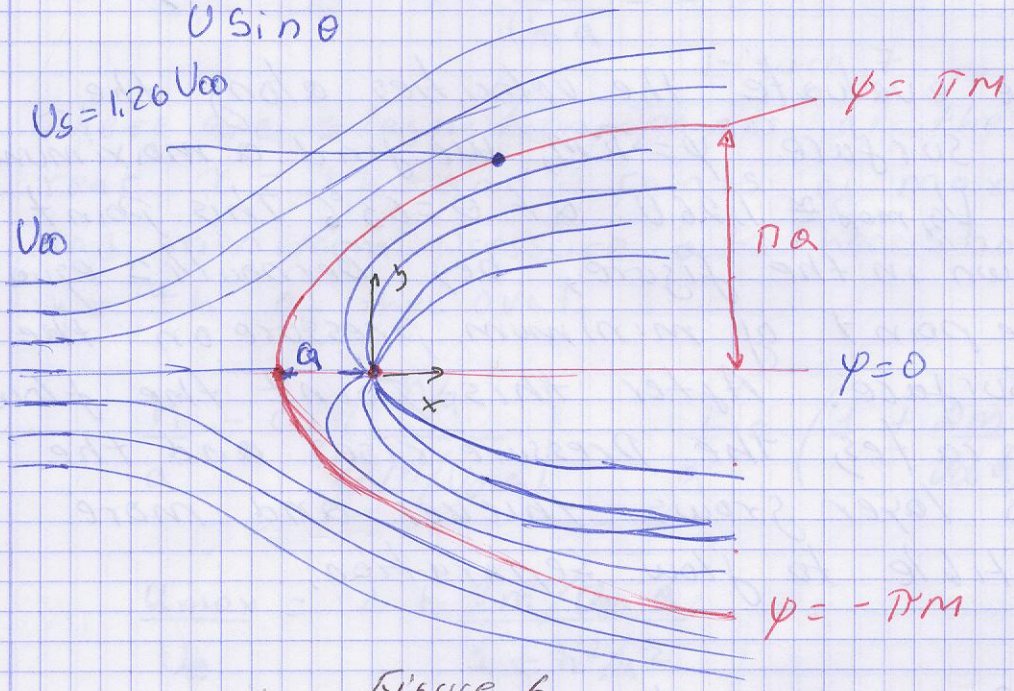

Figure 6

Where $V=0$, stands for $(x, y) = (a, 0)$ where $a = \frac{m}{U}$. the streamline $\psi = 0$ also crosses this point- recall that streamlines can cross only at a stagnation point.

The cartesian velocity components are found by differentiation.

$$u = \frac{\partial \psi}{\partial y} = U + \frac{m}{r}\cos\theta \qquad (12)$$

$$v = -\frac{\partial \psi}{\partial x} = \frac{m}{r}\sin\theta$$

setting $u = v = 0$ we find a single stagnation point at $\theta = 180$ and $r = \frac{m}{U}$

or $(x, y) = (-\frac{m}{U}, 0) \Rightarrow a = \frac{m}{U}$

the resultant of the velocity at any point.

$$V^2 = u^2 + v^2 = U^2\left(1 + \frac{a^2}{r^2} + \frac{2a}{r}\cos\theta\right) \quad (13)$$

If we evaluate the velocities along the upper surface $\psi = \pi m$, we find a maximum value $V_{s,max} \cong 1{,}26U$ at $\theta = 63°$ This point is shown in the figure, bey Bernoulli's equation is the point of minimum pressure on the body surface. After this point the flow decelarates, the pressure rises and the viscous layer grows thicker and more susceptible to flow separation.

The Rankine oval

A cylindrical shape called Rankine oval, which is long compared with its height, is formed by a source-sink pair aligned with a parallel to uniform stream

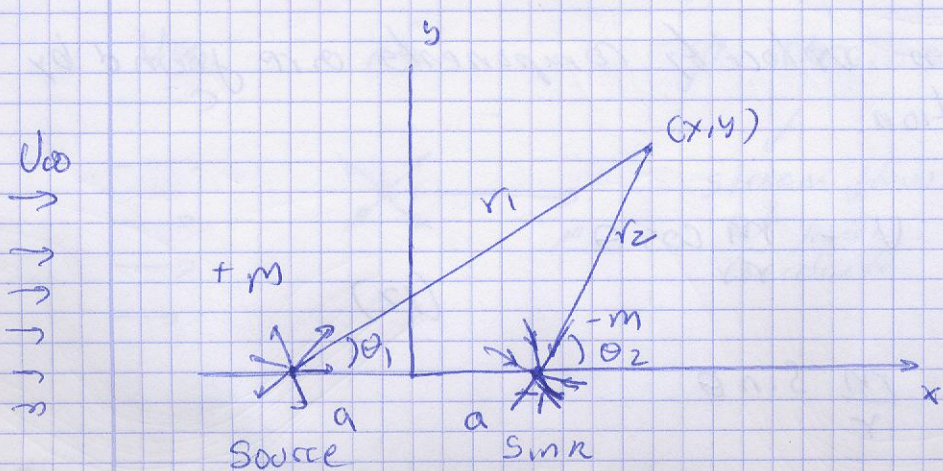

$$\psi = V_\infty y + m\tan^{-1}\left(\frac{2ay}{x^2 + y^2 - a^2}\right) = V_\infty r\sin\theta + m(\theta_1 - \theta_2)$$

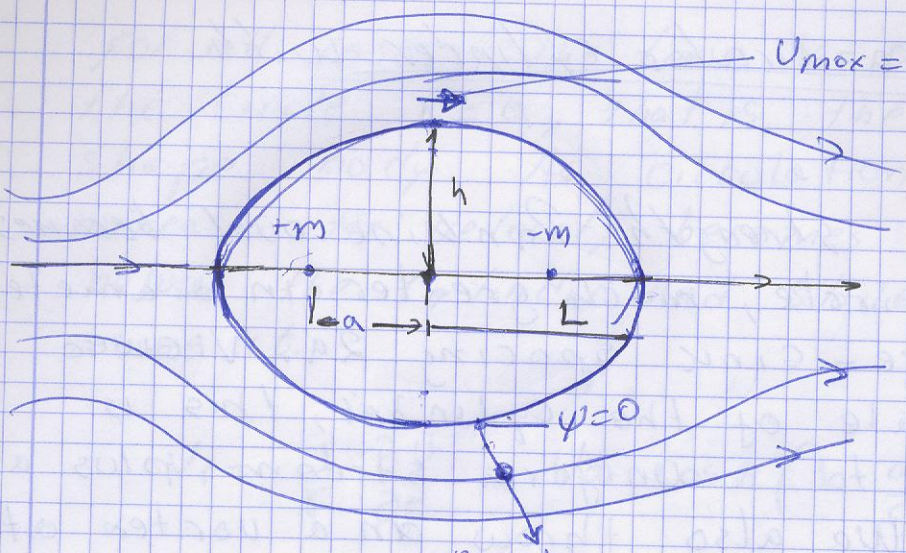

$$\psi = \frac{m}{U_\infty a} = 1$$

Figure 7

There are stagnation points at the front and rear $x = \pm L$ and points of maximum velocity and minimum pressure at the shoulders $y = \pm h$ of the oval.

$$\frac{h}{a} = \cot\left(\frac{h/a}{2m/U_\infty a}\right) \qquad \frac{L}{a} = \left(1 + \frac{2m}{U_\infty a}\right)^{1/2} \tag{14}$$

$$\frac{U_{max}}{U_\infty} = 1 + \frac{2m/U_\infty a}{1 + h^2/a^2}$$

Rankine-oval parameter from (14)

$m/U_\infty a$	h/a	L/a	L/h	U_{max}/U_∞
0	0	1	∞	1
0,01	0,031	1,010	32,79	1,020
0,1	0,263	1,095	4,169	1,187
1	1,307	1,732	1,326	1,789
10	4,435	4,583	1,033	1,968
100	14,130	14,177	1,003	1,992
∞	∞	∞	1	2,00

Flow past a Circular Cylinder with Circulation

At large strength Rankine oval becomes a large circle, much greater in diameter than source-sink spacing $2a$. Viewed on the scale of the cylinder, this is equivalent to a uniform stream plus a doublet. We also throw on a vortex at the doublet center

(15) $$\psi = U_\infty r \sin\theta - \frac{\lambda \sin\theta}{r} - \kappa \ln r + \text{Constant}$$

$\lambda = 2am$ = constant : Doublet strength and unit of velocity times length squared, and for convenience let λ be $U_\infty a^2$ the last Const. Eqvl to $\kappa \ln a$

$$\psi = U_\infty \sin\theta \left(r - \frac{a^2}{r} \right) - \kappa \ln \left(\frac{r}{a} \right) \quad (16)$$

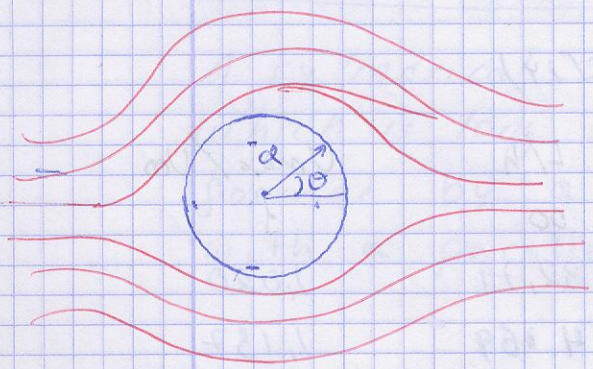

$\frac{\kappa}{U_\infty a} = 0$

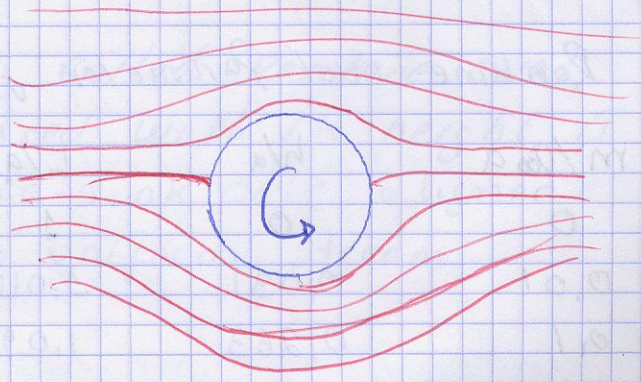

$\frac{\kappa}{U_\infty a} = 1$

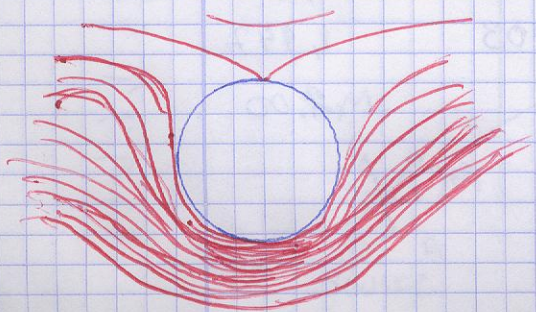

$\frac{\kappa}{U_\infty a} = 2$

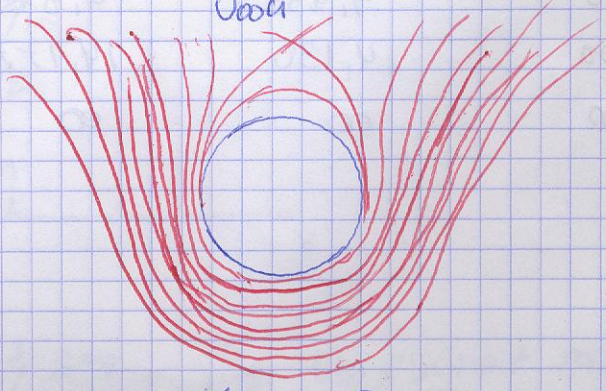

$\kappa = 3$

For all cases the line $\psi = 0$ corresponds to the circle $r = a$, that is, the cylindrical shape body. As circulation $\Gamma = 2\pi K$ increases the velocity becomes faster and faster below the cylindir and slower and slower above it.

$$V_r = \frac{1}{r}\frac{\partial \psi}{\partial \theta} = U_\infty \cos\theta \left(1 - \frac{a^2}{r^2}\right) \qquad (17)$$

$$V_\theta = -\frac{\partial \psi}{\partial r} = -U_\infty \sin\theta \left(1 + \frac{a^2}{r^2}\right) + \frac{K}{r} \qquad (18)$$

The velocity at the cylinder surface $r = a$

$$V_r\big|_{r=a} = 0 \qquad V_\theta\big|_{r=a} = -2U_\infty \sin\theta + \frac{K}{a}$$

For small K, two stagnation points appear on the surface at angles θ_s where $V_\theta = 0$ or

$$\sin\theta_s = \frac{K}{2U_\infty a}$$

for $K = 0$ $\theta_s = 0$ and $\theta_s = 180°$

For $\frac{K}{U_\infty a} = 1$ $\theta_s = 30°$ and $150°$

For $\frac{K}{U_\infty a} = 2$ $\theta_s = 90°$

For $\frac{K}{U_\infty a} > 2$ is invalid and the single stagnation point is above the cylinder.

at the point $y = h$ we have

$$\frac{h}{a} = \frac{1}{2}\left[\beta + (\beta^2 - 4)^{1/2}\right] \qquad \beta = \frac{K}{U_\infty a} > 2$$

$$\frac{h}{a} = 2.6 \quad \text{for} \quad \frac{K}{U_\infty a} = 3.$$

For the cylinder flows there is a downward force, or negative lift called the MAGNUS EFFECTS, which is proportional to stream velocity and vortex strength.

It is seem that, on the top of the cylinder the velocity strength is less than that on the bottom of the cylinder, and therefore, the pressure higher from Bernoulli's equation this explains the force.
There is non-viscous force of course because the theory is inviscid.

From Bernoulli's equation neglecting gravity the surface Pressure P_s is given by

$$P_\infty + \frac{1}{2}\rho V_\infty^2 = P_s + \frac{1}{2}\rho\left(-2V_\infty \sin\theta + \frac{K}{a}\right)^2 \quad (19)$$

$$P_s - P_\infty = \frac{1}{2}\rho V_\infty^2 (1 - 4\sin^2\theta + 4\beta\sin\theta - \beta^2) \quad (20)$$

where $\beta = \frac{K}{V_\infty a}$ and P_∞ is the free-stream Pressure.

If we set up b as the cylinder depth into the paper, the drag D is the integral over the surface of the horizontal component of the pressure force.

$$D = -\int_0^{2\pi} (P_s - P_\infty)\cos\theta \, b a \, d\theta \quad (21)$$

$$D = \sin\theta \int_0^{2\pi} (P_s - P_\infty)\, b a = 0 \quad (22)$$

$$D = (\text{Cylinder with Circulation}) = 0 \quad (23)$$

This is a special case of d'Alembert's paradox.

According to inviscid theory, the drag of any body of any shape immersed in a uniform stream is identically zero

The lift force normal to the stream is given by summation of vertical pressure forces.

$$L = \int_0^{2\pi} (P_s - P_\infty) \cdot \sin\theta \; b a \, d\theta \qquad (24)$$

Since integral over 2π of any odd power of $\sin\theta$ is zero, only the third term in the parentheses in equation (20) contributes to the lift.

$$L = -\frac{1}{2} \rho V_\infty^2 \frac{4K}{a V_\infty} \cdot ba \int_0^{2\pi} \sin^2 d\theta \qquad (25)$$

$$L = -\frac{1}{2} \rho V_\infty (2\pi K) b \quad \text{or} \qquad (26)$$

$$\frac{L}{b} = -\rho V_\infty \Gamma \qquad (27)$$

From (27), the lift is independent of the radius a of the cylinder, the circulation Γ depends upon the body size and orientation through a physical requirement.

Equation (27) was generalized by Kutta in (1902) and independently by Joukowski in (1906) as follows

According to inviscid theory, the lift per unit depth of any cylinder of any shape immersed in a uniform stream equals $\rho V_\infty \Gamma$, where Γ is the total net circulation contained with the body shape. The direction of the lift is 90° from the stream direction, rotating opposite to the circulation

The problem in airfoil analysis, is thus to determine the circulation Γ as a function of airfoil shape and orientation.

Airfoil Theory

The problem is to determine the net circulation Γ as a function of airfoil shape and free-stream angle of attack α.

KUTTA Condition:

Even if the airfoil shape and free-stream angle of attack are specified, the potential flow theory solution is nonunique.

An infinite solutions can be found corresponding to different values of circulation Γ.

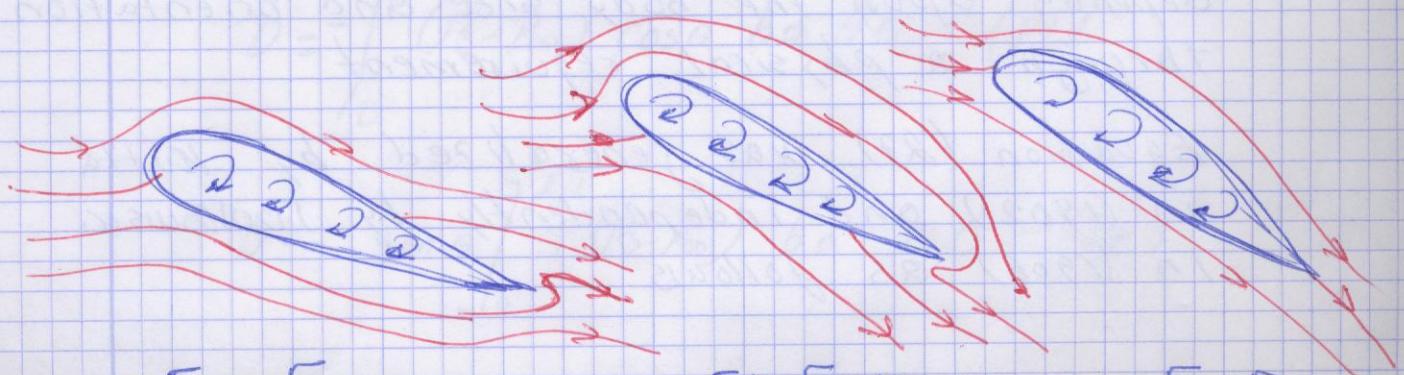

Figure 10

The Kutta condition properly simulates the flow about an airfoil, (a) too little circulation, stagnation point on rear upper surface (b) too much, stagnation point rear lower surface (c) just right Kutta conditions requires smooth flow at trailing edge. In this the upper and lower flow meet and leave the trailing edge smoothly.

If the trailing edge is rounded slightly, there will be a stagnation point there.

If the trailing edge is sharp, approximating most airfoil designs, the upper- and lower surface flow velocities will be equal as they meet and leave the airfoil.

Experiments show that when a body with a sharp trailing edge is set in motion, the action of the fluid viscosity causes the flow over the upper and lower surfaces to merge smoothly at the trailing edge; this circumstance, which fixes the magnitude of the circulation around the body is termed the KUTTA CONDITION..

" A body with sharp trailing edge in motion through a fluid creates about itself a circulation of sufficient strength to hold the rear stagnation point at the trailing edge "

case Flat-plate Airfoil vortex-sheet theory.

Plat-plate is the simplest airfoil, having no thickness or shape but even the theory is not so simple.

To solve the problem, we use a vortex-sheet approach.

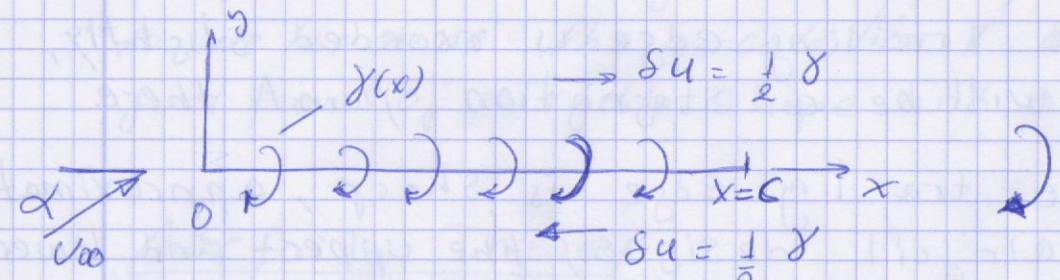

Figure 11

$$u_u - u_L = \gamma(x) \qquad (28)$$

circulation (Γ) at clockwise to make Lift "up"

γ: vortex sheet ~~with~~ of variable strength γ(x).

C: Flat-plate length.

If we omit the free stream, the sheet should cause a rightward flow $\delta u = \frac{1}{2}\gamma(x)$ on the upper surface and opposite leftward flow $\delta u = \frac{1}{2}\gamma(x)$ on the lower surface.

Kutta condition for this sharp trailing edge requires that this velocity difference vanish at the trailing edge to keep the exit flow smooth and parallel

$$\gamma(c) = 0 \qquad (29)$$

The proper solution must satisfy this condition, after which the total lift can be computed by summing the sheet strength over the whole airfoil, for a foil depth 'b'.

$$L = \rho V_\infty b \Gamma \qquad \Gamma = \int_0^c \gamma(x)\, dx \qquad (30)$$

An alternative way to compute lift is from dimensionless pressure coefficient C_p on the upper and lower surfaces

$$C_{pU,L} = \frac{P_{U,L} - P_\infty}{\frac{1}{2}\rho V_\infty^2} = 1 - \frac{U_{U,L}^2}{V_\infty^2} \qquad (31)$$

$$U_{U,L} = (V_\infty \cos\alpha \pm \delta u)^2 + (V_\infty (\sin\alpha))^2$$

This is given combining the uniform stream and vortex-sheet velocity.

$$U_{U,L} = V_\infty^2 \pm 2 V_\infty \delta u \cdot \cos\alpha + \delta u^2 \qquad (32)$$

$$U_{U,L} = V_\infty^2 \left(1 \pm \frac{2\delta u}{V_\infty}\right) \qquad (33)$$

- $\cos\alpha \approx 0$ for small α.
- $\frac{\delta u^2}{V_\infty^2} \ll\ll < 1$

so (31) is given by

$$C_{pU,L} = 1 \pm \left(1 \pm 2\frac{\delta u}{V_\infty}\right) \qquad (34)$$

$$C_{pU,L} = \pm 2\frac{\delta u}{V_\infty} = \pm \frac{\delta}{V_\infty} \qquad (35)$$

The lift force is the integral of the pressure difference over the length of the airfoil, assuming depth b

$$L = \int_0^c (P_L - P_U)\, b\, dx \qquad (36)$$

or

$$(37) \quad C_L = \frac{L}{\frac{1}{2}\rho V_\infty^2 b c} = \int_0^1 (C_{pL} - C_{pU})\frac{dx}{c} = 2\int_0^1 \frac{\gamma}{V_\infty} d\left(\frac{x}{c}\right)$$

Equations (30) and (31) are equivalent within the small-angle approximation

Sheet strength $\gamma(x)$ is computed from the requirement that the net normal velocity $V(x)$ be zero at the sheet ($y=0$).

Considering a small piece of sheet $\gamma\,dx$ located at position x_0, the velocity v at point x on the sheet is that of an infinitesimal line vortex of strength

$$d\Gamma = -\gamma\,dx \qquad (38)$$

$$dv\Big|_x = \frac{d\Gamma}{2\pi r}\Big|_{x_0 \to x} = \frac{-\gamma\,dx}{2\pi(x_0 - x)} \qquad (39)$$

The total normal velocity induced by the entire sheet at point x is thus

$$V\Big|_{sheet} = -\int_0^C \frac{-\gamma}{2\pi(x_0 - x)}\,dx \qquad (40)$$

The uniform stream induces a constant normal velocity at every point on the sheet given by.

$$V_{stream} = U_\infty \sin\alpha$$

Setting the sum of V_{sheet} and V_{stream} equal to zero gives the integral equation

$$\int_0^C \frac{\gamma\,dx}{x_0 - x} = 2\pi U_\infty \sin\alpha \qquad (41)$$

To be solved for $\gamma(x)$ subject to Kutta condition $\gamma(C) = 0$

Equation (41) is quite formidable. In fact it was solved long ago by using integral formulas developed by Poisson in the 1900.

$$\gamma(x) = 2V_\infty \sin\alpha \left(\frac{c}{x} - 1\right)^{1/2} \qquad (42)$$

From eq. (35) the surface pressure coefficient are thus

$$C_{pU,L} = \pm 2 \sin\alpha \left(\frac{c}{x} - 1\right)^{1/2} \qquad (43)$$

Pressure coefficients from (43) are plotted below

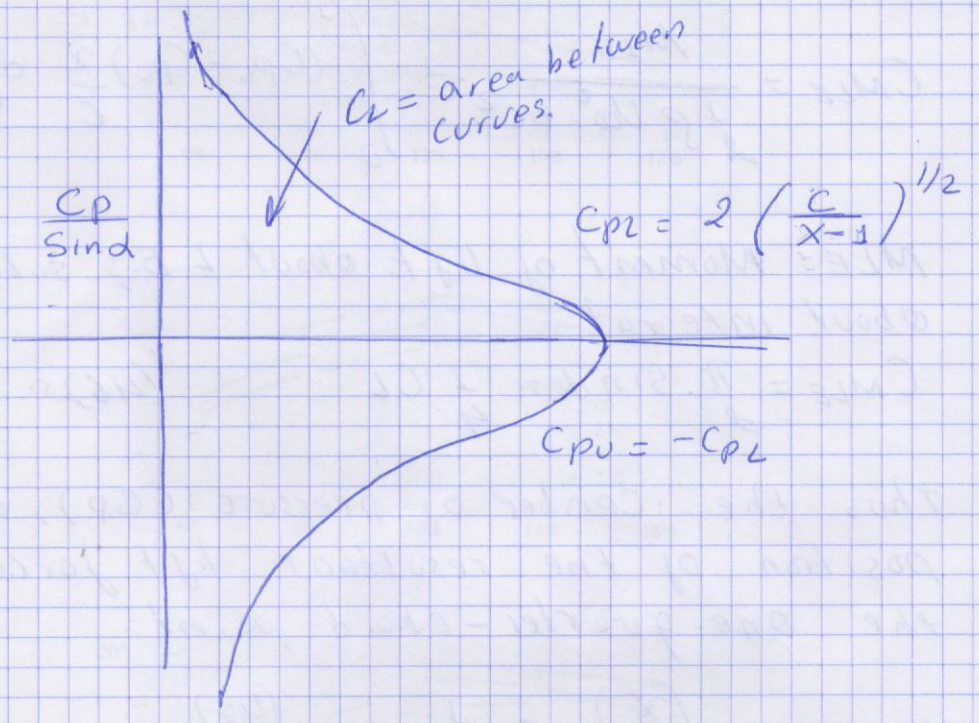

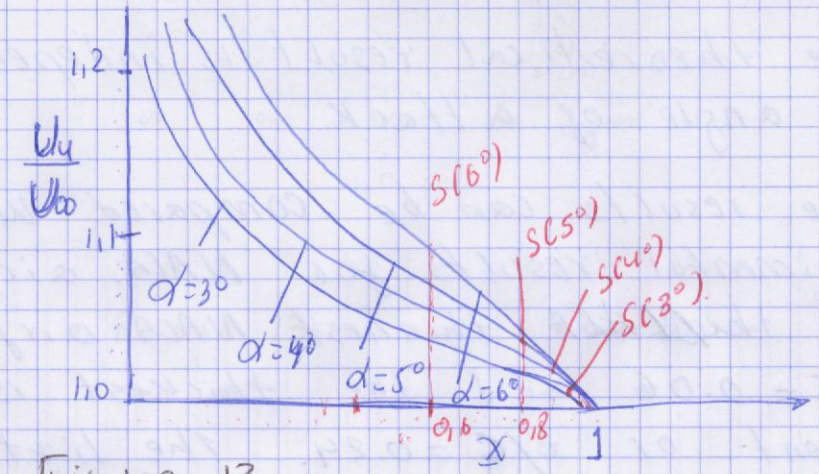

Figure 12

Upper-surface velocity $V_u = V_\infty + \delta u = V_\infty + \frac{1}{2}\gamma$ vs different angle of attack

The lift coefficient of the airfoil is proportional to the area between C_{pL} and C_{pU}

$$C_L = 2\int_0^1 \frac{\gamma}{U}\, d\left(\frac{x}{c}\right) = 4 \sin\alpha \int_0^1 \left(\frac{c}{x} - 1\right)^{1/2} d\left(\frac{x}{c}\right)$$

$$C_L = 2\pi \cdot \sin\alpha = 2\pi\alpha \qquad (44)$$

Also of interest is the momentum coefficient about the leading edge (LE) of the airfoil taken positive counterclockwise

$$C_{M_{LE}} = \frac{M_{LE}}{\frac{1}{2}\rho V_\infty^2 \cdot bc^2} = \int_0^1 (C_{pL} - C_{pU}) \frac{x}{c}\, d\left(\frac{x}{c}\right) \qquad (45)$$

M_{LE} = Moment of lift about L.E.; solving the about integral

$$C_{M_{LE}} = \frac{\pi}{2} \cdot \sin\alpha = \frac{1}{4} C_L \qquad (46)$$

Thus the center of pressure (CP), or position of the resultant lift force, is at the one-quarter-chord point

$$\left(\frac{x}{c}\right)_{cp} = \frac{1}{4} \qquad (47)$$

The theoretical result is independent of the angle of attack.

These results can be compared with experimental results for NACA airfoils. The ~~thickest NACA~~ thinnest NACA airfoil is $t/c = 0.06$ and the thickest is 24 percent or $t/c = 0.24$. The lift-curve slope $dC_L/d\alpha$ is within 9 percent

of the theoretical value of 2π for all the various airfoil families at all thickness.
Increasing thickness tends to increase both $C_{l_{max}}$ and the stall angle.
The stall angle at $t/c = 0.06$ is about $8°$ and would be even less for a flat plate.

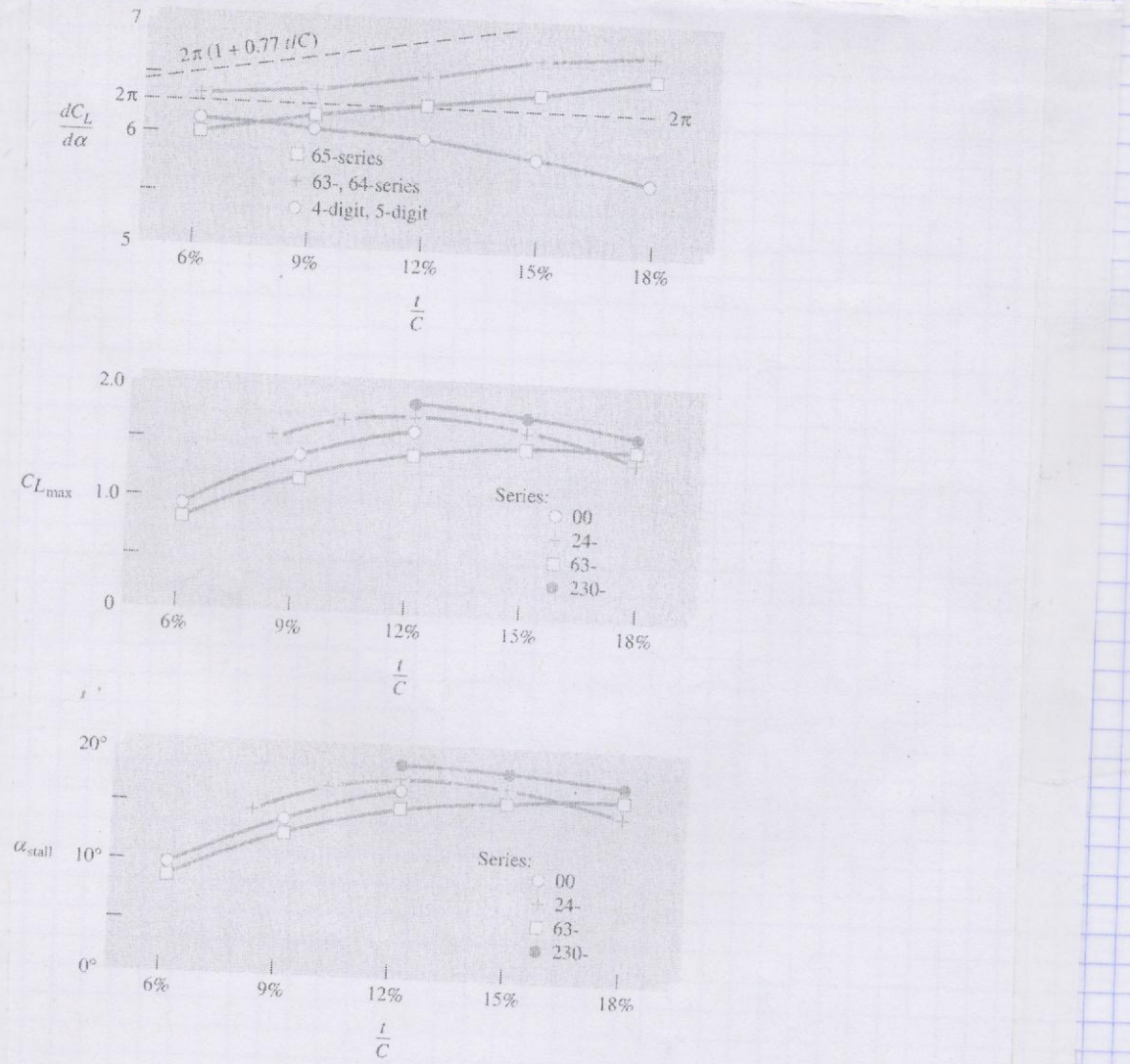

Figure 13

Potential theory for thick cambered airfoils.

Basically the theory uses a complex-variable mapping which transforms the flow about the cylinder with circulation into flow about a foil shape with circulation.

The circulation is then adjusted to match the Kutta condition of smooth exit flow from the trailing edge.

Regardless of exact airfoil shape, the inviscid mapping theory predicts that the correct circulation for any thick cambered airfoil is

$$\Gamma_{Kutta} = \pi b C V_\infty \left(1 + 0{,}77 \frac{t}{C}\right) \sin(\alpha + \beta) \quad (48)$$

where $\beta = \tan^{-1}(2h/C)$ and h is the maximum camber, or maximum deviation of the airfoil midline from its chord line.

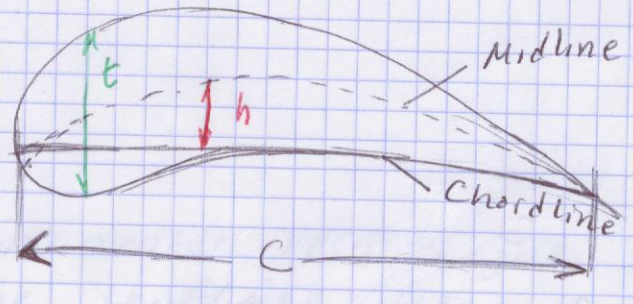

Figure 14

The lift coefficient of infinite-span airfoils is thus

$$C_L = \frac{\rho V_\infty \Gamma}{\frac{1}{2}\rho V_\infty^2 bc} = 2\pi\left(1 + 0{,}77 \frac{t}{C}\right) \sin(\alpha + \beta)$$

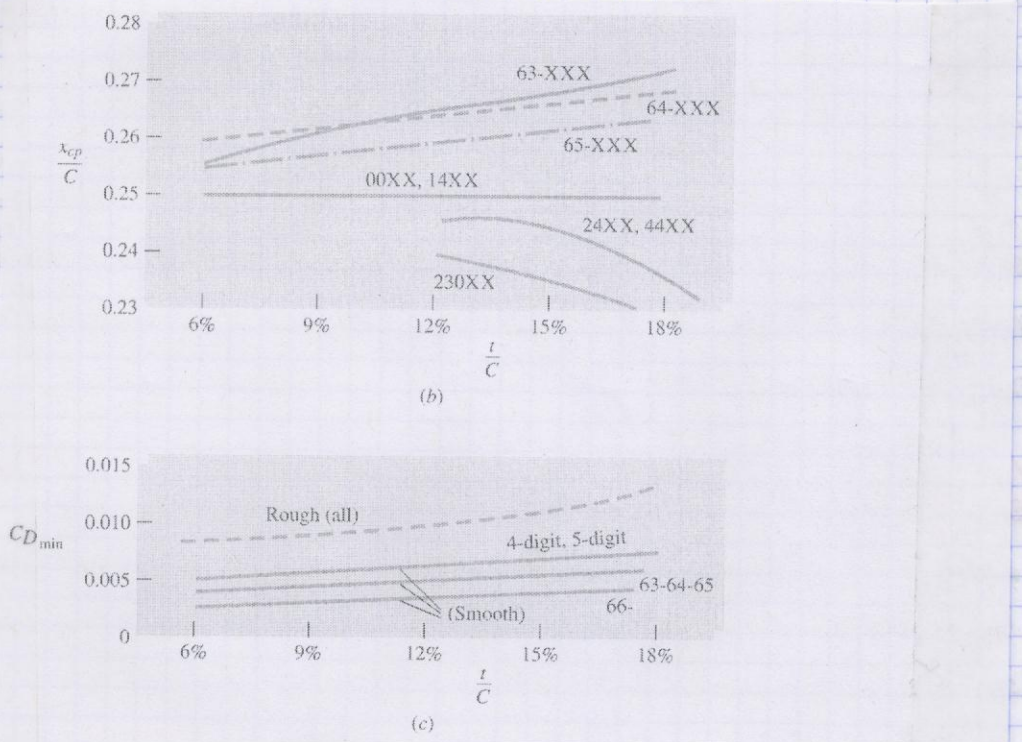

Figure 15
(b). Center-of-Pressure data (c) minimum drag coefficient.

This reduces eq. (44) when thickness and camber are zero, in Figure 13, shows that the thickness effect $1 + 0.77\frac{t}{C}$ is not verified by experiment.
Some airfoil increase lift with thickness, other decrease, and none approach theory very closely,

One reason is the growth of the boundary layer on the upper surface affecting the airfoil shape. Thus it is customary to drop the thickness effect from the theory

$$C_L \simeq 2\pi \sin(\alpha + \beta) \quad (49)$$

The theory correctly predicts that a cambered airfoil will have finite lift at zero angle of attack and zero lift (ZL) at angle.

$$\alpha_{ZL} = -\beta = -\tan^{-1}\left(\frac{2h}{c}\right) \qquad (50)$$

Eq (50) overpredicts the measured zero-lift angle by 1° or so, as shows in the table, the measured values are essentially independent of thickness.

Airfoil series	Camber, % (h/c)	Measured α_{ZL}	Theory $-\beta$, deg
24XX	2.0	-2.1	-2.3
44XX	4.0	-4.0	-4.6
230 XX	1.8	-1.3	-2.1
63-2XX	2.2	-1.8	-2.5
63-4XX	4.4	-3.1	-5.0
64-1XX	1.1	-0.8	-1.2

Wings of Finite Span.

The results of airfoils and experiments of previous analysis of this report, were for two dimensional, or infinite-span, wings. But all real wings have tips and are therefore of finite span or finite aspect ratio AR

$$AR = \frac{b^2}{A_p} = \frac{b}{c} \qquad (51)$$

Where b is the span length from tip to tip and A_p is the planform area of the wings as seen from above.

The lift and drag coefficients of finite-aspect-ratio wing depend upon the aspect ratio and slightly upon the planform shape of the wing.

The vortices cannot end in a fluid, they must either extend to the boundary or form a closed loop.

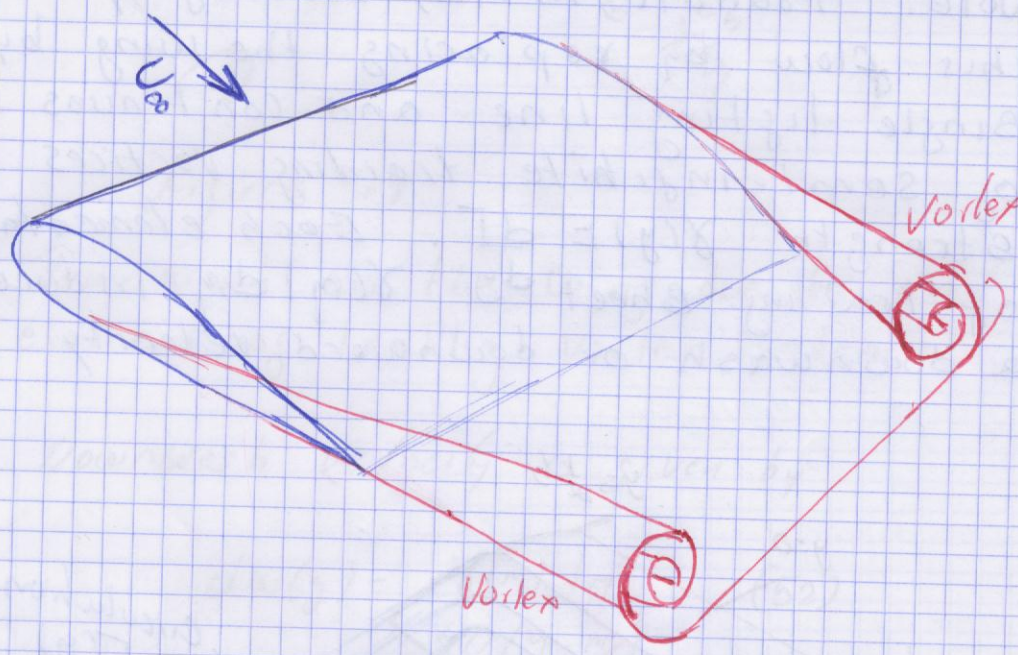

Figure 16.

Shows how the vortices which provide the wing circulation bend downstream at finite wing tips and extend far behind the wing to join to joint the starting vortex. downstream.

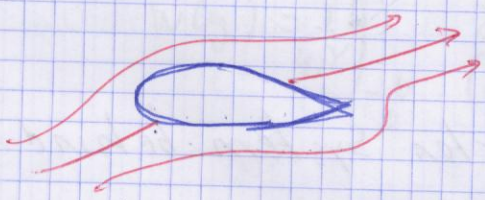

(a) Start-up near stagnation on upper surface. No lift

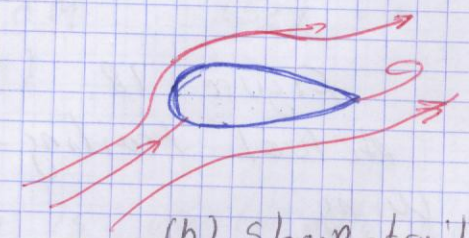

(b) Sharp-trailing edge induces separation and starting vortex sheds. Stream lines flow smoothly. ~~Small~~ Slight Lift

(c) 80% lift developed

(d) Starting vortex now shed behind. Lift fully developed

The strongest vortices are shed from tips, but some are shed from the body of the wing.

The effective circulation $\Gamma(y)$ of these trailing edge shed vortices is zero at the tips and usually a maximum at the center plane, or root, of the wing.

Note: Prandtl, in 1918, succesfully modeled this flow by replacing the wing by a single lifting line and continuos sheet of semi-infinite trailing vortices of strength $\gamma(y) = \frac{d\Gamma}{dy}$. Each elemental piece of trailing sheet $\gamma(\eta)\,d\eta$ induces a downwash or downword velocity $dw(y)$

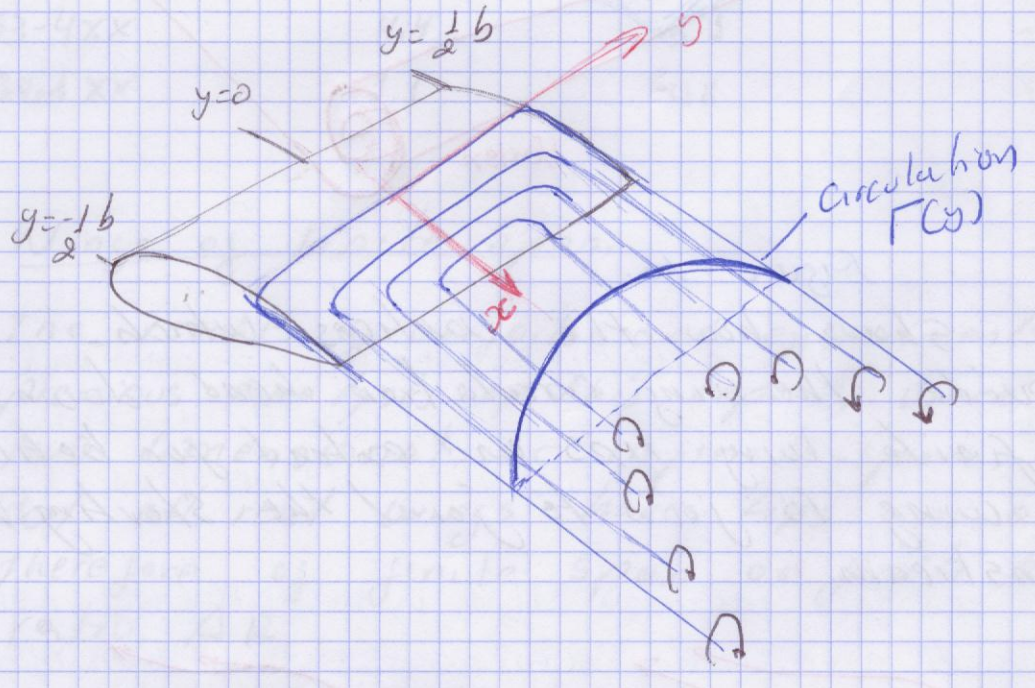

Figure 18.
Actual trailing-vortex system behind wing

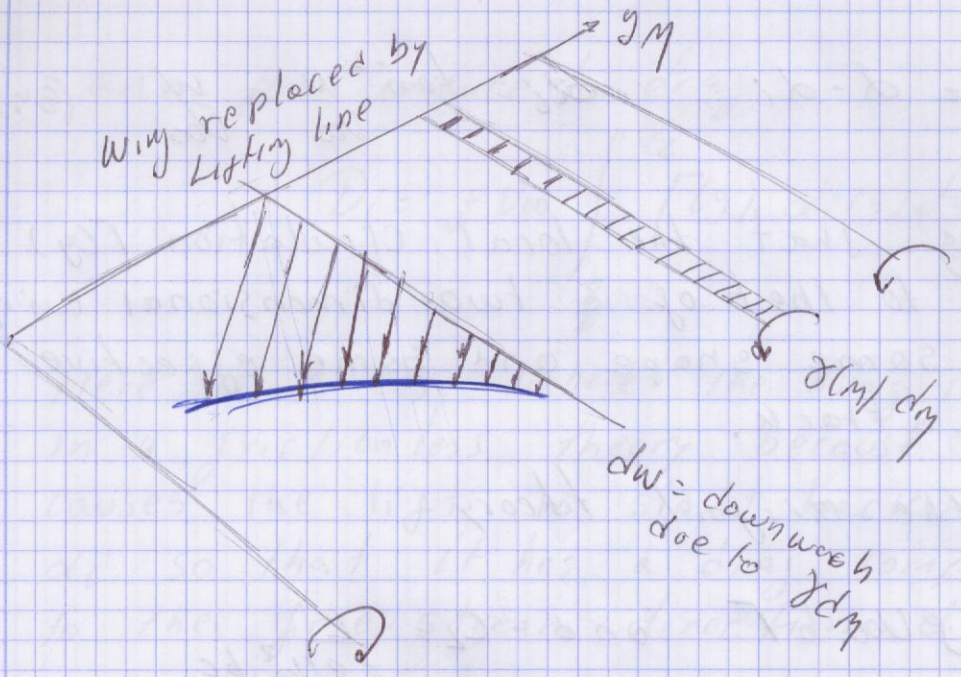

Figure 14

Downwash on the wing due to an element of trailing-vortex system.

The Downwash velocity is given by

$$dw(y) = \frac{\gamma(\eta)\,d\eta}{4\pi(y-\eta)} \qquad (52)$$

at position (y) on the lifting line. The term 4π is because the trailing vortex extends only from 0 to ∞ rather than $-\infty$ to ∞.

The total downwash is obtained by the integral

$$w(y) = \frac{1}{4\pi}\int_{-\frac{b}{2}}^{\frac{b}{2}} \frac{\gamma(\eta)\,d\eta}{(y-\eta)} \qquad (53)$$

When the downwash is vectorially added to approaching free stream V_∞, the effective angle of attack at this section of the wing is reduced to

$$\alpha_{eff} = \alpha - \alpha_i \qquad \alpha_i = \tan^{-1}\frac{w}{V_\infty} = \frac{w}{V_\infty} \qquad (54)$$

Assuming that the local circulation $\Gamma(y)$ is equal to that of a two-dimensional wing of the same shape and same effective angle of attack.

From the airfoil theory

$$L = \rho V_\infty \cdot b\Gamma \quad \text{and} \quad C_L = \frac{L}{\frac{1}{2}\rho V_\infty^2 \cdot bc}$$

$$C_L = \frac{\rho V_\infty \cdot b\Gamma}{\frac{1}{2}\rho V_\infty^2 \cdot bc} \cong 2\pi\alpha_{eff} \qquad (55)$$

and $$\Gamma \cong \pi c V_\infty \alpha_{eff} \qquad (56)$$

Combining (53) and (56). we obtain Prandtl's lifting-line theory for a finite span wing

$$(57) \quad \Gamma(y) = \pi c(y) \cdot V_\infty \left[\alpha(y) - \frac{1}{4\pi V_\infty}\int_{-\frac{b}{2}}^{\frac{b}{2}} \frac{\left[d\Gamma/d\eta\right]d\eta}{y-\eta}\right]$$

this is an integro differential equation to be solved for $\Gamma(y)$ subject to the conditions $\Gamma(-\frac{b}{2}) = \Gamma(\frac{b}{2}) = 0$. It is similar to the thin-airfoil integral equation.

The solution for wing Lift is given by

$$L = \rho V_\infty \int_{-\frac{b}{2}}^{\frac{b}{2}} \Gamma(y)\,dy \qquad (58)$$

and for induced drag

$$D_i = \rho V_\infty \int_{-\frac{b}{2}}^{b/2} \Gamma(y)\, \alpha_i(y)\, dy \qquad (59)$$

Here is a case where the drag is not zero in a frictionless theory because the downwash causes the lift to slant backward by angle α_i so that it has a drag component parallel to the free-stream direction. $dD_i = dL \sin\alpha_i \doteq dL\,\alpha_i$

For arbitrary wing planform $c(y)$ and arbitrary twist $\alpha(y)$ is treated in advance text of aerodynamics.

For an untwisted wing of elliptical planform

$$c(y) = c_0 \left[1 - \left(\frac{2y}{b}\right)^2\right]^{1/2} \qquad (60)$$

The area and aspect ratio of this wing are

$$(61) \qquad A_p = \int_{-\frac{b}{2}}^{\frac{b}{2}} c\, dy = \frac{1}{4}\pi b c_0 \qquad AR = \frac{4b}{\pi c_0}$$

Solving equation (57) we obtain an elliptical circulation distribution of exactly similar shape.

$$\Gamma(y) = \Gamma_0 \left[1 - \left(\frac{2y}{b}\right)^2\right]^{1/2} \qquad (62)$$

we relate Γ_0 and C_0

$$\Gamma_0 = \frac{\pi C_0 V_\infty \alpha}{1 + 2/AR} \quad (63)$$

where α is assumed constant across the untwisted wing.

Substitution into eq. (58) gives the elliptical-wing lift

$$L = \frac{1}{4} \frac{\pi^2 b C_0 \rho V_\infty^2 \alpha}{(1 + 2/AR)} \quad (64)$$

$$C_L = \frac{2\pi\alpha}{1 + 2/AR} \quad (65)$$

If we generalize this to a thick-cambered finite wing of approximately elliptical planform. we obtain.

$$C_L = \frac{2\pi \sin(\alpha + \beta)}{(1 + 2/AR)} \quad (66)$$

From equation (53) the computed downwash for elliptical wing is constant.

$$w(y) = \frac{2 V_\infty \alpha}{2 + AR} = \text{constant.} \quad (67)$$

Finally, the induced drag coefficient from (53).

$$C_{D_i} = C_L \frac{w}{V_\infty} = \frac{C_L^2}{\pi AR} \quad (68)$$

The below figure shows the effectiveness of this theory when tested against a nonelliptical cambered wing by Prandtl. (a) and (b) shows measured lift curves and drag polars for five different aspect ratios.

Note, the increase in stall angle and drag and decrease in lift slope as the aspect ratio decreases.

(c) shows the lift data replotted against effective angle of attack $\alpha_{eff} = \frac{\alpha + \beta}{(1 + 2/AR)}$ as it is predicted by eq. (66)

These curves should be equivalent to an infinite-aspect ratio wing, and they do collapse together except near stall.

Their common slope $dC_L/d\alpha$ is about 10% less than the theorical value 2π but this is consistent with the thickness and shape effects noted in figure 13.

(d) shows the drag data replotted with the theoretical induced drag $C_{Di} = C_L^2/\pi AR$ subtracted out. Again, except near stall the data collapse onto a single line nearly constant infinite-aspect-ratio drag $C_{D0} = 0.01$.

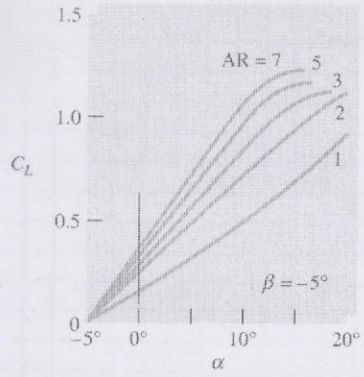
1.5
1.0
0.5
0
C_L
AR = 7
5
3
2
1
$\beta = -5°$
−5°
0°
10°
20°
α

(a)

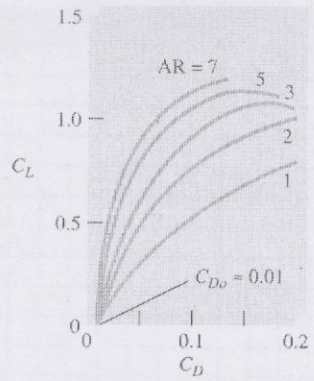
1.5
1.0
0.5
0
C_L
AR = 7
5
3
2
1
$C_{Do} = 0.01$
0
0.1
0.2
C_D

(b)

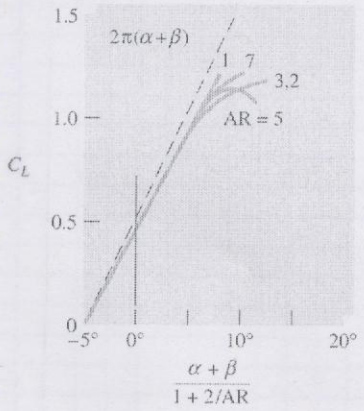
1.5
1.0
0.5
0
C_L
$2\pi(\alpha+\beta)$
1
7
3.2
AR = 5
−5°
0°
10°
20°
$\frac{\alpha+\beta}{1+2/\text{AR}}$

(c)

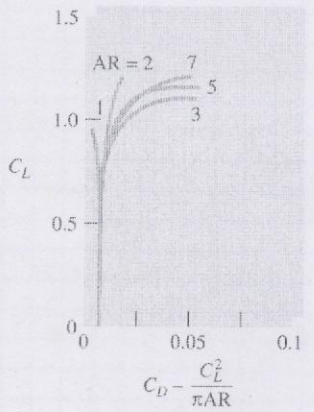
1.5
1.0
0.5
0
C_L
AR = 2
7
5
3
1
0
0.05
0.1
$C_D - \frac{C_L^2}{\pi \text{AR}}$

(d)